JOURNAL OF VIROLOGY, Apr. 2003, p. 3939–3949 Vol. 77, No. 7
0022-538X/03/$08.00+0 DOI: 10.1128/JVI.77.7.3939–3949.2003

The Leader of Human Immunodeficiency Virus Type 1 Genomic RNA Harbors an Internal Ribosome Entry Segment That Is Active during the G_2/M Phase of the Cell Cycle

Ann Brasey,[1] Marcelo Lopez-Lastra,[1] Theophile Ohlmann,[2] Nancy Beerens,[3] Ben Berkhout,[3] Jean-Luc Darlix,[2] and Nahum Sonenberg[1]*

Biochemistry Department, McGill University, H3G 1Y6 Montréal, Canada[1]; LaboRetro, INSERM U 412, École Normale Supérieure de Lyon, 69364 Lyon Cedex 07, France[2]; and Department of Human Retrovirology, Academic Medical Center, University of Amsterdam, 1105AZ Amsterdam, The Netherlands[3]

Received 10 September 2002/Accepted 10 January 2003

The 5′ leader of the human immunodeficiency virus type 1 (HIV-1) genomic RNA contains highly structured domains involved in key steps of the viral life cycle. These RNA domains inhibit cap-dependent protein synthesis. Here we report that the HIV-1 5′ leader harbors an internal ribosome entry site (IRES) capable of driving protein synthesis during the G_2/M cell cycle phase in which cap-dependent initiation is inhibited. The HIV-1 IRES was delineated with bicistronic mRNAs in in vitro and ex vivo assays. The HIV-1 leader IRES spans nucleotides 104 to 336 and partially overlaps the major determinants of genomic RNA packaging. These data strongly suggest that, as for HIV-1 transcription, IRES-mediated translation initiation could play an important role in virus replication during virus-induced G_2/M cell cycle arrest.

The 5′ leader of human immunodeficiency virus type 1 (HIV-1) genomic RNA is comprised of multiple functional elements that are critical for virus replication (10). They are involved in transcription, mRNA splicing, genomic RNA dimerization, encapsidation, and reverse transcription. The structure of the HIV-1 leader has been studied extensively, revealing that most of the elements consist of stable stem-loop structures (7, 10, 12). Some of the structures inhibit viral mRNA translation (22, 67, 78).

Translation of most eukaryotic mRNAs is thought to occur by a scanning mechanism, whereby the 40S ribosomal subunit binds in the vicinity of the mRNA 5′ cap structure and scans in the 5′ to 3′ direction until an initiation codon in an appropriate sequence context is encountered (40). This process involves a number of initiation factors. The cap structure is bound by eIF4F, which is a three-subunit complex composed of eIF4E, the cap-binding protein, eIF4A, which possesses RNA-dependent helicase activity, and eIF4G, a modular scaffolding protein, which bridges the mRNA cap (via eIF4E) and the 40S ribosomal subunit (via eIF3). Studies of picornavirus translation were the first to reveal an alternative mechanism of translation initiation by internal ribosome binding, which is mediated by an internal ribosome entry segment (IRES) (46, 71). A major difference in the mechanism of cap-dependent versus internal ribosome binding is that eIF4E is dispensable for the latter. Consistent with this, the carboxy-terminal 2/3 fragment of eIF4G, which lacks the eIF4E binding site, is sufficient to promote internal initiation (64).

The mRNAs from retroelements and several members of the *Retroviridae*, including HIV-1, initiate translation via an IRES (5, 15, 16, 19, 31, 52, 53, 62, 80). Most IRESs characterized so far, from both viral and cellular origins, reside upstream of the open reading frame (ORF). This location is consistent with the 5′ to 3′ direction of ribosome scanning. Among the few exceptions is HIV-1 (19), where the presence of an IRES was reported within the *gag* ORF. The same study concluded that this IRES (here referred to as the 40K IRES) drives translation initiation from the upstream *gag* initiation codon. This suggests that upon recruitment to the *gag* ORF, the 40S ribosomal subunit translocates in a 3′ to 5′ direction to recognize the initiation codon of *gag*. This observation prompted us to undertake studies in order to understand this unusual backward-scanning model of translation initiation (68, 79, 82).

Here we identified a novel IRES present within the 5′ leader of HIV-1 (HIV-1 IRES). We show that this IRES overlaps the primer binding site, the dimer initiation site, the major splice donor, and the major determinants of the encapsidation signal (ψ) that are located upstream from the HIV-1 *gag* initiation codon (3, 7, 10, 25, 27, 39, 51, 57). Moreover, the HIV-1 IRES functions during the G_2/M phase of the cell cycle, demonstrating that the IRES fulfills an important function during HIV-1 replication.

MATERIALS AND METHODS

Plasmid constructions. For generation of bicistronic constructs, fragments of HIV-1 were amplified by PCR from plasmid pNL4-3 (2), digested with *Eco*RI and *Nco*I (PCR-added restriction sites), and inserted into the intercistronic region of a dual luciferase reporter plasmid (a kind gift from P. Sarnow) (83). All HIV inserts were verified by sequence analysis. To generate the Moloney murine leukemia virus-based retroviral vector MLV-Plap-HIV-1(1-336)-neo, the HIV-1 leader (positions 1 to 336) generated by PCR and digested with *Nhe*I (site added with the PCR primer) was cloned between the placental alkaline phosphatase (*Plap*) and neomycin phosphotransferase (*neo*) genes of pMLV-CB71 (15). A poliovirus IRES dual luciferase reporter construct was obtained by subcloning the *Renilla* luciferase gene into the *Nhe*I and *Xba*I sites, the poliovirus IRES into

* Corresponding author. Mailing address: Biochemistry Department, Room 807, McIntyre Medical Sciences Building, McGill University, 3655 Promenade Sir William Osler, H3G 1Y6 Montréal, Canada. Phone: (514) 398-7274. Fax: (514) 398-1287. E-mail: nahum.sonenberg@mcgill.ca.

the *Hin*dIII and *Eco*RV sites, and the firefly luciferase gene into the *Bam*HI and *Xho*I sites of the pcDNA3 backbone (Invitrogen).

pHIVCG4 and cyclin plasmids were described previously (63). Monocistronic constructs were generated as follows. The pHIVCG4 plasmid, encoding the proviral DNA from HIV-1 MAL (4), was linearized at the *Ssp*I site, generating the template for the HIV-*gag* mRNA starting at the +1 transcription site and coding for *gag*-p55. Capped cyclin B2 mRNA was generated by linearizing pXL-EMCV with *Bam*HI. The encephalomyocarditis virus IRES was amplified by PCR and inserted into pMLV-CB93 previously digested with *Nhe*I (15) to create pEMCV-LacZ.

For mutation of the primer-binding site region, pBlue-5′LTR (50), which contains an *Xba*I-*Cla*I fragment of HIV-1 encompassing the 5′ long terminal repeat, the primer-binding site, and the 5′ end of the *gag* gene (positions −454 to +376) was inserted into pBluescript (Stratagene). The central primer-binding site-stem region was extended by oligonucleotide-directed in vitro mutagenesis with a Muta-Gene phagemid in vitro mutagenesis kit (Bio-Rad). The oligonucleotides used were S1 (5′-$^{+118}$TGTGTGACTCTGGT-*TT*-CCCTTTTAGTCA GTG^{+164}-3′) and S2 (5′-$^{+208}$GAAAGGGAAACCAGAG-*TC*-ACGCAGGA CTCGGCT^{+249}-3′) (the position of the deletion is marked by dashes, and the 2-nucleotide insertion is in italics). The deletions introduced were verified by sequence analysis. Subsequently, the mutated *Xba*I-*Cla*I fragments were introduced into the proviral clone pLAI-R37, a derivative of the full-length infectious clone pLAI (11), which was also verified by sequence analysis. Evidence was previously presented for the folding of these structures in vitro and ex vivo (8). For the ornithine decarboxylase IRES control, the ornithine decarboxylase 5′ untranslated region (nucleotides 1 to 303) was subcloned from CAT-303-LUC (73) into the aforementioned dual luciferase reporter plasmid.

Cell culture. HeLa, COS-7, and TeFly-A cells (29, 32) were cultured in Dulbecco's modified Eagle's medium (Gibco-BRL) with 50 U of penicillin-streptomycin/ml and 10% fetal bovine serum at 37°C in a 5% CO_2 atmosphere. C33A cells were grown in Dulbecco's modified Eagle's medium containing 10% fetal bovine serum at 37°C and 5% CO_2. To cause G_2/M arrest, HeLa cells were incubated for 18 h in medium containing 0.4 μg of nocodazole per ml (Sigma-Aldrich).

Preparation of translation extracts. HeLa cells were trypsinized and resuspended in Dulbecco's modified Eagle's medium containing 10% fetal bovine serum and 50 U of penicillin-streptomycin/ml. Cells were collected by centrifugation at 710 × *g* for 5 min and washed three times in phosphate-buffered saline (137 mM NaCl, 2.7 mM KCl, 4.3 mM $Na_2HPO_4 \cdot 7H_2O$, 1.4 mM KH_2PO_4, pH 7.4) at 4°C. Cell pellets were resuspended in 2 volumes of hypotonic buffer (10 mM HEPES-KOH [pH 7.6], 10 mM potassium acetate, 0.5 mM magnesium acetate, 1 mM dithiothreitol) and incubated for 5 min on ice. Cells were disrupted by passing 20 to 30 times through a 1.5-in. (ca. 3-cm) 23-gauge needle. The final potassium acetate concentration was adjusted to 50 mM. Cells were then centrifuged at 16,000 × *g* for 10 min at 4°C. Following micrococcal nuclease treatment, the extract was centrifuged at 16,000 × *g* for 5 min at 4°C. The resulting supernatant was passed through NICK columns (Amersham Pharmacia Biotech) and eluted with elution buffer (10 mM HEPES-KOH [pH 7.6], 50 mM potassium acetate, 0.5 mM magnesium acetate, 2 mM dithiothreitol). Creatine kinase (Calbiochem) was added at 0.2 U per microliter of extract. Protein concentration was determined by the Bio-Rad assay, and the extract was divided into aliquots, frozen in liquid nitrogen, and stored at −80°C.

In vitro transcription. Capped and uncapped mRNAs were synthesized with T7 RNA polymerase (mMessage mMachine kit from Ambion and enzyme-buffer set from MBI) according to the manufacturer's protocol. Plasmid DNA (1 to 2 μg) linearized with *Bam*HI was used for RNA synthesis in a 20-μl or 50-μl final volume for capped and uncapped RNAs, respectively. The template DNA was digested with DNase I, and RNA was precipitated with 7.5 M LiCl. RNA was resuspended in 20 μl of diethyl pyrocarbonate-treated water. RNA concentrations were determined spectrophotometrically and adjusted to 0.1 mg/ml. RNA integrity was monitored by agarose gel electrophoresis.

In vitro translation. For the bicistronic constructs, in vitro translations were typically carried out in a final volume of 22 μl containing HeLa translation extract (40.5 μg of protein), 20 μM amino acids, 8 mM creatine phosphate, 20 mM HEPES-KOH buffer, pH 7.6, 1 mM ATP, 0.2 mM GTP, 0.5 mM spermidine, and potassium acetate in the range of 80 to 150 mM, magnesium acetate in the range of 0.3 to 1.25 mM, and RNA in the range of 50 to 335 ng, as indicated in the figure legends. Translation reactions were incubated at 30°C for 90 min. Luciferase activity was measured with the dual-Luciferase reporter assay system from Promega on a Lumat LB 9507 luminometer from Berthold Technologies. For the monocistronic constructs, capped RNAs were translated in a nuclease-treated rabbit reticulocyte lysate (Promega) in the presence of KCl (75 mM), $MgCl_2$ (0.5 mM), 2-aminopurine (15 mM), and 20 μM each amino acid (except methionine). Preparation of in vitro-translated L protease was carried out as described previously (63). The mixture was incubated for 1 h at 30°C in the presence of 0.6 mCi of [^{35}S]methionine per ml. Translation products were resolved by sodium dodecyl sulfate-polyacrylamide gel electrophoresis (SDS-PAGE), and the gel was dried and subjected to autoradiography for 12 h with Biomax films (Kodak). Bands were quantified with a Storm 850 phosphoimager.

Transfection and Western blot analysis. HeLa cells were grown to 60% confluency in six-well tissue culture dishes and transfected with a total of 1.25 μg of DNA with Lipofectin (Invitrogen) following the manufacturer's protocol. The transfected DNA solution was composed of equal amounts of LacZ reporter plasmid and HIV-1 bicistronic construct. Twenty-eight hours posttransfection, cells were harvested for the luciferase assay according to the manufacturer's protocol (Promega). The protein content of all samples was determined by Bio-Rad assays. Transfection efficiency of each sample was estimated by measuring β-galactosidase activity. Enzymatic activity was determined spectrophotometrically (420 nm) by monitoring the β-galactosidase-mediated hydrolysis of *o*-nitrophenyl-β-D-galactopyranoside (ONPG) to *o*-nitrophenol.

C33A cells were grown in 20 ml of culture medium in a 75-cm^2 flask to 60% confluency and transfected by the calcium phosphate method (23). Forty micrograms of the proviral construct in 880 μl of water was mixed with 1 ml of 50 mM HEPES-KOH (pH 7.1)–250 mM NaCl–1.5 mM Na_2HPO_4–120 μl of 2 M $CaCl_2$, incubated at room temperature for 20 min, and added to the culture medium. The culture medium was changed after 16 h. Three days posttransfection, the cells were washed with phosphate-buffered saline and lysed in 0.5 ml of reducing SDS sample buffer (50 mM Tris-HCl [pH 7.0], 2% SDS, 10% β-mercaptoethanol, 5% glycerol). Proteins were resolved in a 10% SDS-polyacrylamide gel and transferred to Immobilon-P (16 h, 60 V). The membrane was blocked with Tris-buffered saline (TBS: 100 mM Tris-Cl [pH 7.5], 150 mM NaCl) containing 5% nonfat dry milk and 0.05% Tween 20, and incubated with serum of an HIV-1-infected individual (patient H) for 1 h at room temperature. Subsequently, the membrane was washed with TBS containing 0.5% Tween 20 and incubated with goat anti-human immunoglobulin G-alkaline phosphatase conjugate. Finally, the membrane was washed with TBS containing 0.5% Tween 20 and developed with the 5-bromo-4-chloro-3-indolylphosphate–nitroblue tetrazolium protocol (Sigma).

Proteins 15 μg extracted from cycling and nocodazole-treated HeLa cells stably transduced with the MLV-Plap-HIV-1(1-336)-neo construct (15 μg) were resolved in a 12.5% SDS-polyacrylamide gel and transferred to a 0.45-μm Protran nitrocellulose membrane (Schleider and Schuell) for 2 h at 70 V. The membrane was blocked with phosphate-buffered saline containing 0. 5% Tween 20 and 5% nonfat dry milk. Blots were then incubated with anti-neomycin phosphotransferase II polyclonal antibody (Cortex Biochem, Inc.) or antiactin monoclonal antibody (Sigma) and visualized by enhanced luminescence (Amersham Life Sciences). To determine the induction of protein expression, films were visualized with an Image Reader LAS-1000 Plus system (FujiFilm) and quantified with Image Gauge version 3.3.

Flow cytometry. Cells were trypsinized, rinsed twice with 1 ml of cold phosphate-buffered saline, and fixed in 80% ethanol–phosphate-buffered saline for 30 min at 4°C. Phosphate-buffered saline (2 volumes) was added, and cells were pelleted by slow centrifugation. Cells were rinsed twice with 2 ml of phosphate-buffered saline, resuspended in 0.5 ml of phosphate-buffered saline containing 0.2 μg of RNase A per ml, and incubated for 40 min at 37°C. Propidium iodide was added to a final concentration of 1.2 μg/ml, and samples were analyzed by fluorescence-activated cell sorting (FACS) with a single-laser FACS instrument (Becton Dickinson) combined with the CellQuest software.

Transfection, infection, and recombinant virus titration. TeFly-A helper cell lines (29, 32) were seeded at 5 × 10^5 cells per 100-mm plate 24 h prior to transfection with 20 μg of the MLV-Plap-HIV-1(1-336)-neo retroviral vector DNA by the calcium phosphate method (23). Upon transfection, cells were selected with 0.8 mg of G418 per ml. G418-resistant clones were mixed, expanded, and used for recombinant virus production. For vector titration, COS-7 cells were seeded 24 h prior to transduction at 2 × 10^4 cells per well in a 24-well plate. Freshly harvested virus-containing medium was filtered (0.45-μm pore size filter). Serial dilutions of this supernatant were overlaid onto cells in the presence of 4 μg of Polybrene per ml. Cells were then incubated for 24 h, after which the medium was replaced. Cells were fixed and stained for the expression of Plap protein.

The recombinant viral titer was determined by counting the number of Plap-positive cells 48 h postinfection in limiting-dilution infections of COS-7 cells. Titer, as transducing units per milliliter, was calculated as (number of colonies) × (dilution of infecting retrovirus)/(total volume in milliliters of diluted vector overlaid onto cells). HeLa cells were seeded at 5 × 10^5 cells per 100-mm plate 24 h prior to transduction. Harvested virus from stably expressing TeFly-A helper

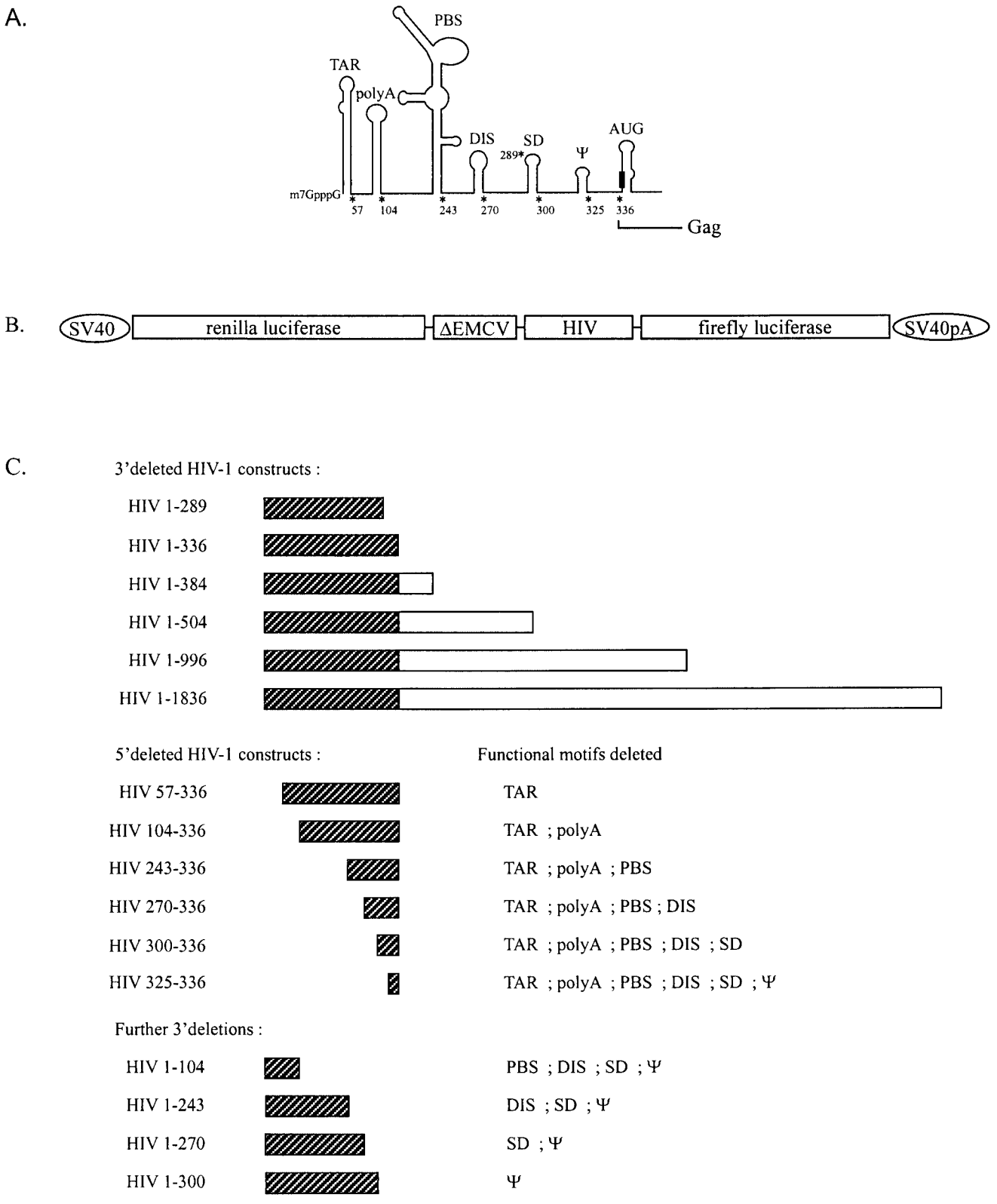

FIG. 1. Design of bicistronic HIV-1 plasmids. (A) Schematic representation of the functional domains in the HIV-1 5′ leader. The RNA 5′ leader region contains the *trans*-activation-responsive region (TAR), the poly(A) hairpin, the primer binding site (PBS), the dimer initiation site (DIS), the major splice donor (SD), the core packaging signal (ψ), and a hairpin containing the initiator AUG (AUG loop). The asterisks denote the start and end points of deletion mutations that were used in this study. The black box represents the initiator AUG. Adapted from Berkhout (10). (B) Schematic representation of the dual luciferase reporter plasmid used in this study. The different HIV-1 fragments were subcloned into the intercistronic region as described in Materials and Methods. ΔEMCV is the encephalomyocarditis virus IRES which contains an inhibitory deletion (24, 83). (C) PCR-generated fragments of HIV-1 used in this study. The hatched boxes represent leader sequences; the white boxes represent *gag* coding region sequences.

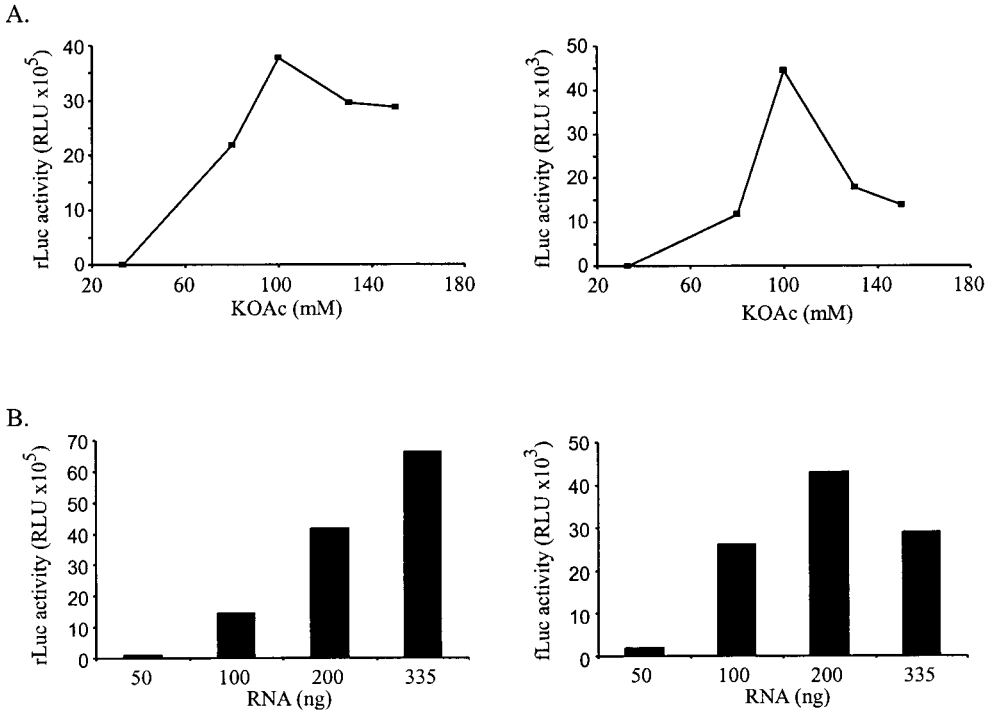

FIG. 2. Optimization of a HeLa cell in vitro translation system. Effect of potassium acetate (KOAc, A) on translation of *Renilla* (rLuc) and firefly luciferase (fLuc) ORFs (first and second cistrons, respectively). RLU, relative light units. (B) RNA dose-response. The RNA contains the full-length HIV-1 5′ leader (nucleotides 1 to 336).

cells were filtered (0.45-μm pore size filter). Vector-containing supernatants at a titer of 0.8×10^6 transducing units/ml (titer established in COS-7 cells) were overlaid onto HeLa cells in the presence of 4 μg of Polybrene per ml. Cells were then incubated at 37°C and 5% CO_2 for 24 h, after which the medium was replaced. Transduced cells were grown for 48 h and subsequently passaged and placed under G418 selection at 0.5 to 0.8 mg/ml.

Human placental alkaline phosphatase staining. Cells were fixed in phosphate-buffered saline containing 2% formaldehyde and 0.2% glutaraldehyde. After two washes in phosphate-buffered saline, cells were incubated at 65°C for 30 min in phosphate-buffered saline. Cells were washed twice with AP buffer (100 mM Tris-HCl [pH 9.5], 100 mM NaCl, and 50 mM $MgCl_2$ in distilled deionized water) and stained with AP buffer containing 0.1 mg of 5-bromo-4-chloro-3-indolylphosphate (BCIP) (Promega) per ml, 1 mg of nitroblue tetrazolium salt (Promega) per ml, and 1 mM levamisole (Sigma).

Metabolic labeling and trichloroacetic acid precipitation. Cycling and nocodazole-treated HeLa cells stably transduced with the MLV-Plap-HIV-1(1-336)-neo construct were metabolically labeled with 11 μCi of [^{35}S]methionine per ml for 30 min. Cells were lysed in 20 mM HEPES-KOH, pH 7.2, containing 5 mM EDTA, 100 mM KCl, 0.005% SDS, 0.5% Elugent, 10% glycerol, 20 mg of chymostatin per ml, and 2 mM microcystin. After a 10-min incubation on ice, cellular debris was removed via centrifugation at 12,000 × *g* for 5 min at 4°C. Proteins were resolved in an SDS–12.5% polyacrylamide gel and visualized after autoradiography. Labeled proteins (50 μg) were precipitated with cold 10% trichloroacetic acid and collected on glass microfiber filters (934-AH from Whatman). Filters were rinsed two times with cold 10% trichloroacetic acid and twice with absolute ethanol and dried overnight at room temperature. Radioactivity was determined in a Beckman LS 3801 scintillation counter.

RESULTS

Determination of boundaries of HIV-1 IRES in vitro. A HeLa cell-free in vitro translation system was used to study the translation initiation mechanism of HIV-1. HeLa extracts were chosen because their addition to a rabbit reticulocyte lysate is required for efficient translation of HIV-1 mRNA (78). The in vitro translation system was optimized with respect to RNA loading and salt conditions with a bicistronic vector containing the HIV-1 leader (Fig. 1A) inserted between the ORFs of the *Renilla* luciferase and firefly luciferase genes (Fig. 1B). In these experiments, firefly luciferase activity serves as the readout for the putative HIV-1 IRES activity. To ensure that the two cistrons are independently translated, a defective encephalomyocarditis virus IRES, known to inhibit ribosome reinitiation and readthrough, was inserted upstream of the HIV-1 leader (24, 83). Figure 2 shows that translation driven by the HIV-1 leader in a bicistronic mRNA was substantial in extracts programmed with 200 ng of RNA at 100 mM potassium acetate. Therefore, the viral leader is a good candidate for harboring an IRES element. Results shown below support this conclusion. Thus, we will refer to this sequence as an IRES from here on.

To determine the 3′ boundary of the IRES, a series of bicistronic constructs containing the 5′ leader plus different portions of the *gag* coding region were examined (Fig. 1C). In other retroviruses and retroelements, except for the reticuloendotheliosis type A virus (52), the IRES spans the packaging signal (15, 53, 80). Since the HIV-1 packaging signal extends into the *gag* coding sequence (54, 58) and Buck et al. reported the existence of an HIV 40K IRES in the *gag* ORF (19), various *gag* ORF segments were also examined. The results from translation of capped and uncapped RNAs demonstrate that maximal translation activity was conferred solely by the 5′ leader of HIV-1 (Fig. 3A, right panel, construct 1-336), excluding the need for any coding sequence. On the contrary, inclusion of *gag* coding regions reduced the translation activity of the HIV-1 leader (compare construct 1-336 with 1-384, 1-504,

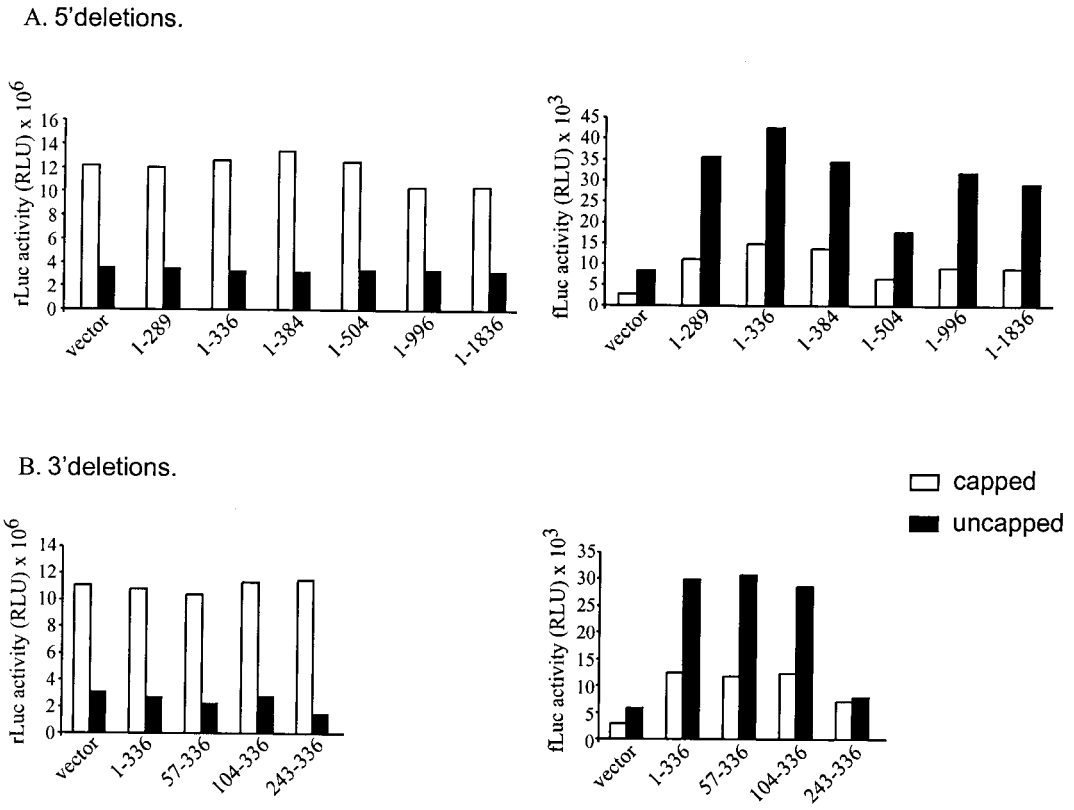

FIG. 3. HIV-1 IRES activity in a HeLa in vitro translation extract. Bicistronic capped and uncapped mRNAs were translated in a HeLa extract as described in Materials and Methods. *Renilla* luciferase and firefly luciferase activities (left and right panels, respectively) of the 3′-deleted HIV-1 constructs (A) and part of the 5′-deleted constructs (B) are shown. The results are from a representative experiment. See the legend to Fig. 2 for abbreviations.

1-996, and 1-1839). Luciferase assays also confirmed that in all constructs, the two ORFs were independently translated, since capping of the mRNA increased expression of the first cistron by about 3.6-fold, while the expression of the second cistron decreased by about 3-fold (Fig. 3A, left panel).

To determine the 5′ boundary of the HIV-1 IRES, a new panel of bicistronic constructs were generated (Fig. 1C). In vitro translation assays with capped and uncapped RNAs showed that deletion of the *trans*-activation-responsive region (construct 57-336) and poly(A) (construct 104-336) hairpin loops had no significant effect on the IRES activity (Fig. 3B, right panel). However, deletion of the primer-binding site hairpin loop (construct 243-336) resulted in a marked decrease (≈6-fold) in activity (Fig. 3B, right panel). Based on these observations, we conclude that the minimal IRES is contained within a 233-nucleotides region spanning nucleotides 104 to 336.

HIV-1 IRES activity in cell culture. Next, the ex vivo activity of the IRES was studied (Fig. 4). In these experiments, a *lacZ* reporter was cotransfected into HeLa cells together with the IRES-containing bicistronic construct to normalize for transfection efficiency. Levels of *Renilla* luciferase and firefly luciferase activity were normalized against protein content and LacZ activity. In agreement with the in vitro assays, the ex vivo data also mapped the minimal IRES element to nucleotides 104 to 336 (Fig. 4, right panel, bar 12, compare with bars 19, 20, 21, and 22). As was observed above, deletion of the *trans*-activation-responsive region (Fig. 4, bar 11) and poly(A) (Fig. 4, bar 12) hairpin loops had no significant effect on the IRES activity. The in vitro data suggest that deletion of the primer-binding site hairpin loop was deleterious to the HIV-1 IRES activity (Fig. 3B, right panel, construct 243-336). Strikingly, this deletion completely abrogated IRES activity (Fig. 4, right panel, bar 13). As expected, further 5′ to 3′ deletions did not restore IRES activity (Fig. 4, lanes 14 through 16), showing that termination-reinitiation is not taking place.

In agreement with the in vitro data, the presence of the *gag* coding sequence reduced IRES activity (compare Fig. 4, bar 4, to bars 5 through 8). In these experiments, cap-dependent translation was enhanced relative to the control vector (compare Fig. 4, bar 2, to bars 3 through 8). This might be explained by an enhancement of mRNA stability or competition between the two cistrons when *gag* coding regions are part of the constructs. The reduction of IRES activity observed in the constructs 1-384, 1-504, 1-996, and 1-1836 (Fig. 4, compare bar 4 to bars 5 through 8) suggests that the *gag* coding region inhibits IRES activity. Possible mechanisms for this inhibition are addressed in the Discussion. Taken together, our data show that the HIV-1 IRES overlaps several functional domains in the HIV-1 leader (Fig. 1A), including the primer-binding site, dimer initiation site, splice donor, and ψ (10).

HIV-1 IRES-dependent translation occurs in the presence of

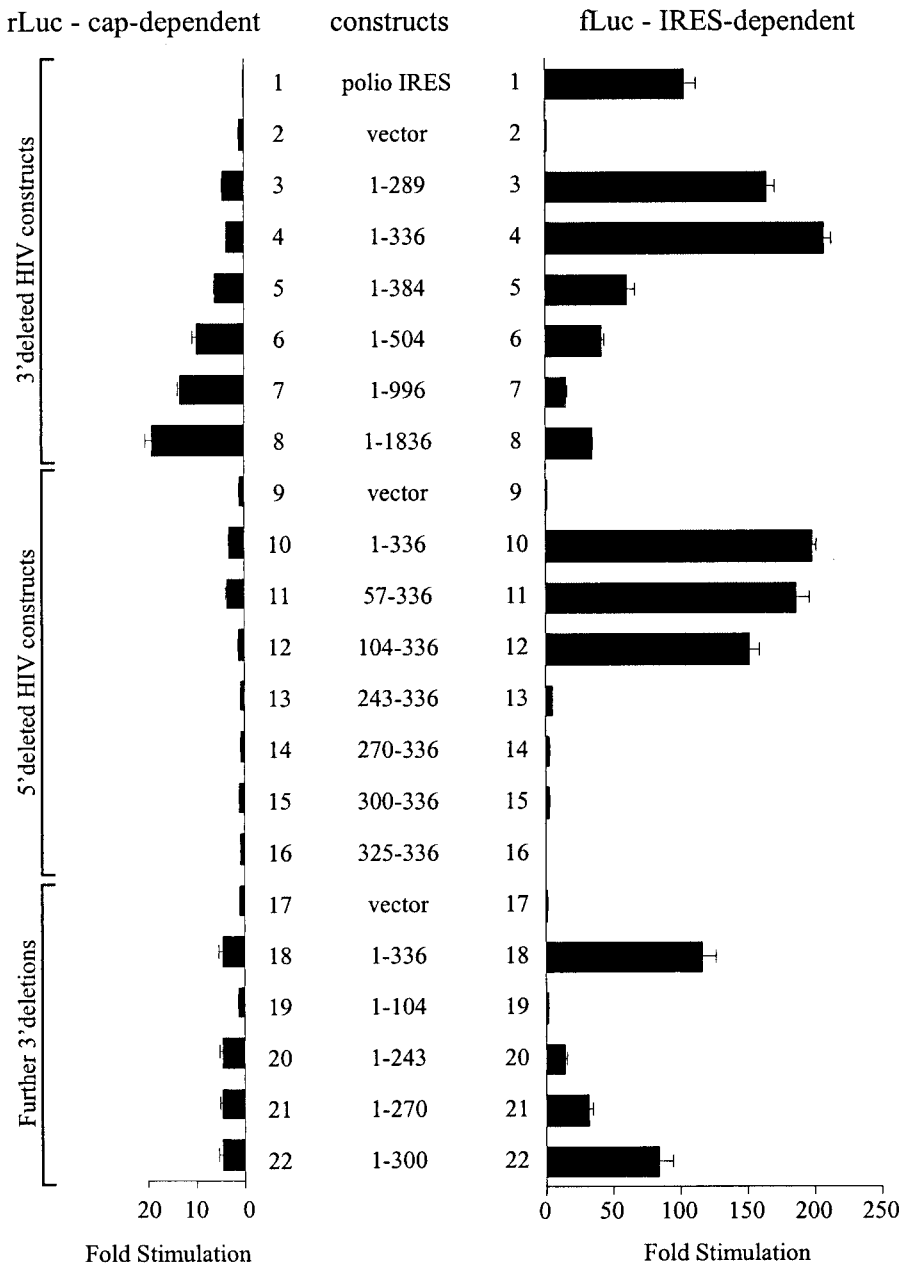

FIG. 4. Demarcation of the HIV-1 IRES. *Renilla* luciferase (rLuc) and firefly luciferase (fLuc) activity (left and right panels, respectively) in HeLa cells 28 h after transient cotransfection with the LacZ reporter and HIV-1 constructs. The results are from a representative experiment performed in triplicate and are expressed as stimulation of translation relative to the control vector. The results did not vary by more than 10%.

cleaved eIF4G. To study the HIV-1 IRES in its natural sequence context, we examined the impact of eIF4G cleavage on the translation of a monocistronic mRNA which contains the full-length HIV-1 leader and the *gag* coding sequence. The L protease from foot-and-mouth disease virus cleaves eIF4G into an N-terminal (one third of the molecule) and a C-terminal (two thirds of the molecule) domain. This proteolytic cleavage results in inhibition of cap-dependent translation, while IRES-driven translation is unaffected or sometimes even stimulated (64).

Translation of the capped HIV-1 mRNA was performed in a rabbit reticulocyte lysate that was previously optimized for simian immunodeficiency virus (SIV) IRES activity (62). The encephalomyocarditis virus IRES was used as a control for IRES-dependent translation, while cyclin B2 mRNA was used as a control for cap-dependent translation (Fig. 5A). As expected, L protease reduced cyclin B2 translation in a dose-dependent manner (Fig. 5B, compare bar 7 with bars 8 and 9), while under the same conditions, encephalomyocarditis virus IRES-mediated translation was unaffected (Fig. 5B, compare bar 4 with bars 5 and 6). Translation of the HIV-1 mRNA was not inhibited by the protease treatment (Fig. 5B, compare bars

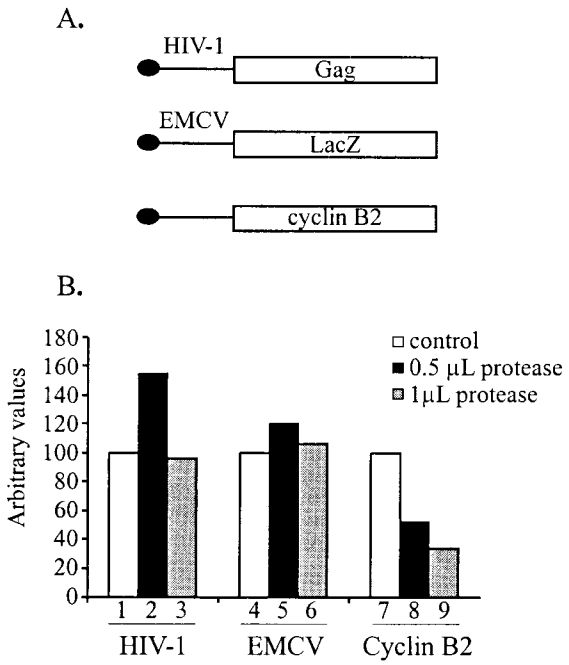

FIG. 5. HIV-1 IRES-driven translation functions with proteolytically cleaved eIF4G. Monocistronic capped RNAs from HIV-1, encephalomyocarditis virus (EMCV), and cyclin B2 (A) were in vitro translated in a rabbit reticulocyte lysate treated with the foot-and-mouth disease virus L protease as previously described (52, 53, 62, 64). [^{35}S]methionine-labeled proteins were subjected to SDS-PAGE and quantified (B) as described in Materials and Methods.

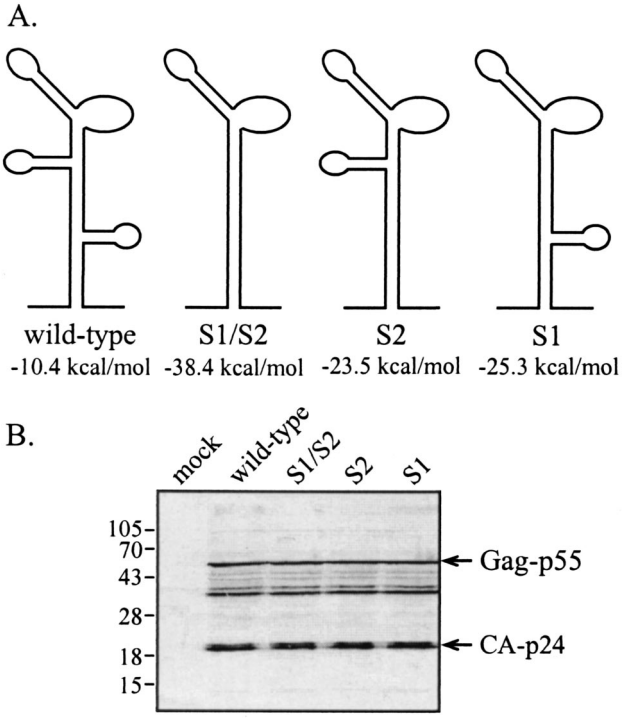

FIG. 6. Increased secondary structure in the primer-binding site region does not inhibit translation. C33A cells were transfected with the wild-type or mutant proviral constructs shown in panel A. Total cellular extracts were prepared 3 days posttransfection, and viral proteins were detected by Western blotting with serum from an HIV-1-infected individual (B). The positions of the HIV-1 *gag*-p55 precursor protein and the mature CA-p24 protein are indicated on the right. Positions of molecular size markers are indicated on the left (in kilodaltons).

1 with 2 and 3). These results show that the HIV-1 IRES functions when positioned upstream of the *gag* sequence.

Mutations which stabilize secondary structure in the HIV-1 leader do not affect viral mRNA translation. One of the hallmarks of an IRES is its insensitivity to increased secondary structure, which potently inhibits cap-dependent translation (70). Thus, the central domain of the full-length HIV-1 leader was mutated to generate RNA secondary structures with increased stability. A short RNA duplex is formed in the wild-type leader region by base-pairing of sequences flanking the primer-binding site (10). This 7-bp duplex of the wild-type HIV-1 RNA was extended to 16 or 15 consecutive base pairs in mutants S1 and S2, respectively. In addition, an S1/2 double mutant able to fold into an uninterrupted RNA duplex of 24 bp was constructed. The free energies (ΔG) predicted by the MFold program (85) for these RNA structures were −10.4 kcal/mol (wild-type), −25.3 kcal/mol (S1 mutant), −23.5 kcal/mol (S2 mutant), and −38.4 kcal/mol (S1/2 mutant) (Fig. 6A). The last value greatly exceeds the stability of the wild-type HIV-1 leader, including that of the extended *trans*-activation-responsive region hairpin structure (−26.2 kcal/mol), which is known to strongly inhibit translation initiation (67, 78). Following transfection in C33A cells, the expression of viral proteins was analyzed by Western blotting. Introduction of very stable RNA structures had no effect on $Pr55^{Gag}$ and CA-p24 protein expression (Fig. 6B). Thus, the HIV-1 IRES is functional in the context of a provirus.

HIV-1 IRES activity is increased in G_2/M-arrested cells in vitro and ex vivo. The activity of several viral and cellular IRESs is increased in the G_2/M phase of the cell cycle, while general cap-dependent translation initiation is suppressed (18, 72). The HIV-1 protein Vpr causes cell growth arrest at G_2/M (34, 35, 56). Vpr upregulates HIV-1 replication during infection of dividing T cells and primary macrophages as a result of its cell cycle-arresting activity (38, 77). It is during this cell cycle arrest that transcription of viral full-length RNA is enhanced (37). Based on these observations, we anticipated that the HIV-1 IRES would be functional during virus-induced G_2/M cell cycle arrest, playing a key role in the replication of HIV-1.

To assess this hypothesis, bicistronic RNAs containing the HIV-1 IRES were translated in HeLa extracts prepared from either nocodazole-treated, cell cycle-arrested or cycling cells. The cell cycle arrest was verified by flow cytometry (Fig. 7A and B). The ornithine decarboxylase IRES, which is known to be active in G_2/M (73), was used as a positive control, while the vector plasmid served as a negative control. As expected, cap-dependent translation was severely inhibited (≈90%) in extracts prepared from nocodazole-treated cells (Fig. 7C). Under these conditions, translation from the HIV-1 IRES and ornithine decarboxylase IRES increased relative to nonarrested cells by 3.1- and 2.2-fold, respectively (Fig. 7D; compare bars 4 to 3 and 6 to 5). These data demonstrate that the HIV-1 IRES

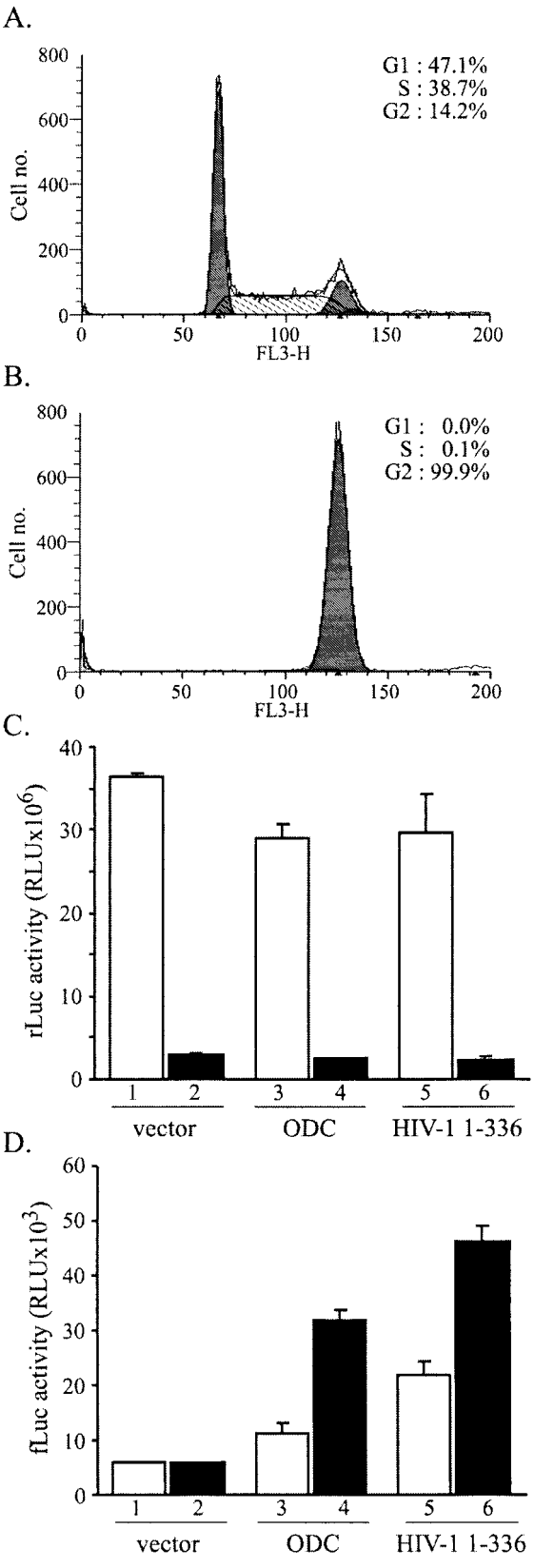

FIG. 7. HIV-1 IRES is active in translation extracts prepared from mitotic cells. FACS analysis of untreated (A) and nocodazole-treated (B) HeLa cells from which in vitro translation extracts were prepared. In vitro translation of bicistronic capped mRNA in untreated (□) and nocodazole-treated (■) HeLa cell extracts (C and D). The values are averages from two independent experiments. The difference in the translation efficiencies of the extracts was normalized by setting the firefly luciferase activity of the negative control vector plasmid to an equal value. See the legend to Fig. 2 for abbreviations.

exhibits increased activity in translation extracts prepared from cells arrested in the G_2/M phase of the cell cycle.

To extend the in vitro results, ex vivo experiments were also performed. HeLa cells stably transduced with a Moloney murine leukemia virus-based retroviral vector, MLV-Plap-HIV(1-336)-neo, were treated with nocodazole. In this system, neomycin levels reflect the HIV-1 IRES activity. The cell cycle state was examined by FACS analysis (Fig. 8A and B). As reported previously (18, 72), metabolic labeling demonstrated that general translation was decreased (53%) in G_2/M-arrested cells (Fig. 8C). In agreement with the in vitro data, translation of the neomycin protein was increased in G_2/M-arrested cells relative to interphase cells (Fig. 8D, compare lane 3 to 2). The amount of actin served as a control for total protein loading. As an equal amount of protein was loaded and actin is a stable protein, its relative concentration was not expected to vary significantly in G_2/M-arrested cells. Taken together, our data demonstrate that the HIV-1 IRES is active during the G_2/M phase of the cell cycle, suggesting that control of translation initiation might have an important role in HIV-1 replication.

DISCUSSION

We showed that the 5′ leader of HIV-1 contains a functional IRES. The boundaries of the minimal IRES lie between nucleotides 104 and 336 of the leader sequence (where +1 corresponds to the 5′ cap of the genomic RNA) (Fig. 1, 3, and 4). The IRES overlaps important functional elements: primer-binding site, dimer initiation site, the major splice donor, and Ψ (3, 7, 10, 25, 27, 39, 51, 57). The *trans*-activation-responsive region and poly(A) loops are not included in the IRES (Fig. 1, 3, and 4). In contrast to picornaviruses (9, 69, 71) and insect picornavirus-like viruses (83), which contain an IRES but do not possess a 5′ cap structure, retroviral mRNAs do contain this structure. Thus, the retroviral mRNAs should be able to translate by a cap-dependent and IRES-mediated mechanism. This dual translation initiation mechanism suggests that the control of translation initiation of HIV-1 full-length mRNA is an important step in the viral life cycle. It might allow HIV-1 to control its gene expression during the different stages of its replication cycle.

The HIV-1 protein Vpr promotes cell differentiation, enhances HIV-1 replication in nondividing macrophages, and blocks proliferating $CD4^+$ T cells at the G_2 cell cycle checkpoint (38, 77). The last property of Vpr enhances viral replication, because HIV-1 transcription is more active during G_2 (37). Similarly, poly(A) polymerase activity and consequently RNA polyadenylation are increased by Vpr (59). However, as cap-dependent translation initiation is suppressed during the G_2/M phase of the cell cycle (72, 74), an increase in viral RNA transcription by itself cannot explain the higher virus yields observed in G_2/M-arrested cells (37). Therefore, IRES-medi-

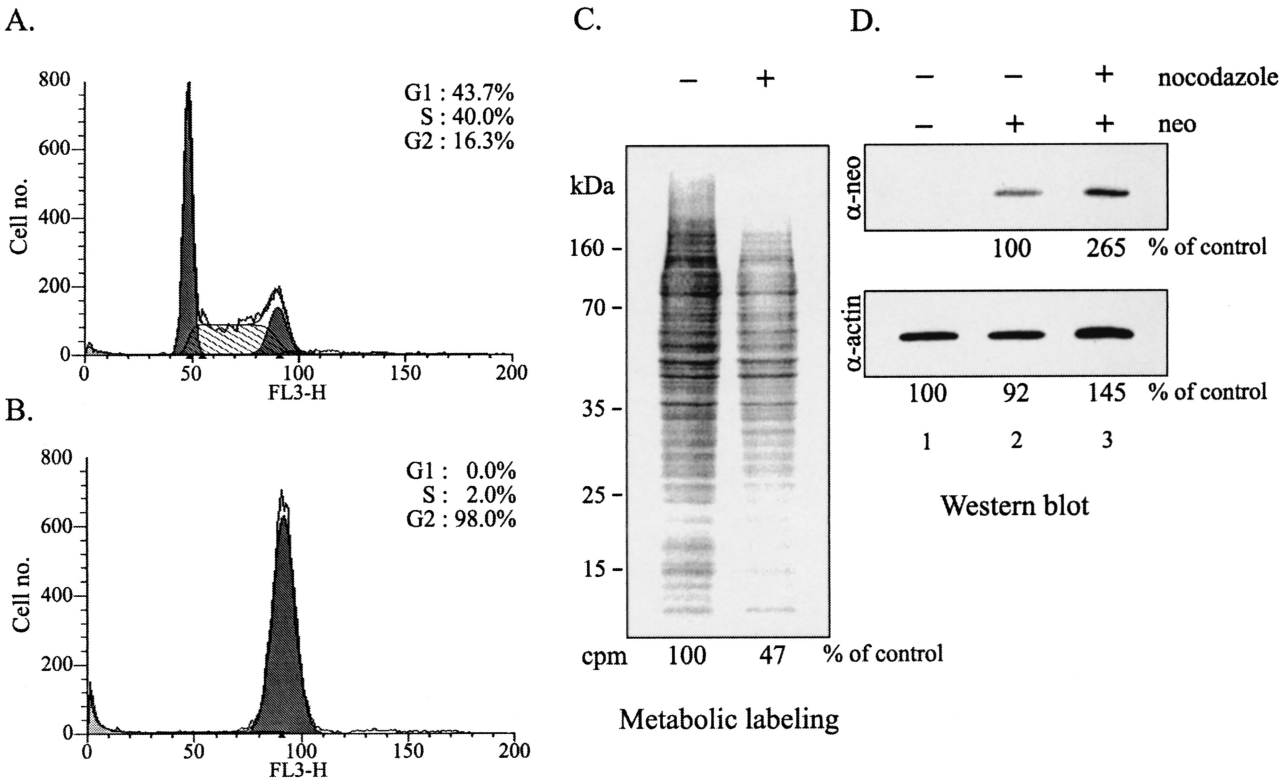

FIG. 8. HIV-1 IRES functions ex vivo in G_2/M-arrested HeLa cells. FACS analysis of untreated (A) and nocodazole-treated (B) HeLa cells which express P*lap*/*neo* as described in Materials and Methods. (C) [^{35}S]methionine-labeled proteins were resolved by SDS-PAGE and visualized by autoradiography. (D) Western blotting for neomycin and actin proteins was performed as described in Materials and Methods. Experiments were repeated three times, and the results of a representative experiment are shown. The results did not differ by more than 20%.

ated translation initiation ensures translation of Gag and Gag-Pol proteins during G_2/M and plays an active role during HIV-1 replication. Thus, our results, together with those of Goh et al. (37), support the hypothesis that virus production is maximized by arresting infected cells in a stage of the cell cycle in which transcription directed by the viral long terminal repeat and Gag polyprotein translation are optimal. The ability to translate at the G_2/M phase has also been described for hepatitis C virus (41), some members of the *Picornaviridae* (18), and the cellular mRNAs for ornithine decarboxylase, c-Myc, and p58^{PITSLRE} (28, 60, 73).

An earlier report by Buck et al. showed that the *gag* ORF also possesses an IRES, which is responsible for the synthesis of a 40-kDa Gag isoform (19). The initiation codon for this novel Gag isoform maps within the *gag* open reading frame. Buck et al. suggest that this 40K IRES is also responsible for translation initiation of the upstream *gag* AUG (19). Were this indeed the case, it would suggest that upon recruitment to the IRES, the 40S ribosomal subunit scans in a 3′ to 5′ direction to encounter the upstream *gag* AUG. The possibility of mRNA backscanning has already been discussed (68, 79, 82) but has not been demonstrated biochemically. In contrast, our data suggest that translation of the Gag polyprotein is mediated by a traditional upstream IRES, which is consistent with the position of IRESs for other retroviruses (15, 31, 52, 62, 80).

The data presented here are not in variance with those of Buck et al. but might reveal a new degree of complexity to the HIV-1 translation initiation process. This is not without precedent, as multiple IRESs which are present within a single transcriptional unit have been described for c-*myc* (61), vascular endothelial growth factor (42), and cricket paralysis virus (83) mRNAs. Interestingly, for cricket paralysis virus and c-*myc*, each IRES drives the translation of a separate ORF (61, 83).

A long-standing question in retrovirus replication is how mRNA translation is coordinated with genomic RNA packaging, since these two processes are conflicting and cannot occur at the same time for a given RNA molecule (20). Two copies of the genomic RNA are encapsidated, linked at their 5′ end through the dimer initiation site (13, 65, 66, 76). The specificity of RNA packaging is determined by two components, (i) the *cis*-acting ψ signal and (ii) the Gag polyprotein, which binds the viral genomic RNA. Mutational analysis of the nucleocapsid (NC) domain of *gag* demonstrated the importance of this domain for encapsidation of viral genomic RNA (6, 14, 26, 30, 48, 49, 55, 75, 81, 84).

In HIV-1, the full-length RNA acts both as mRNA and as genomic RNA (21, 33, 47). A change in the folding of the 5′ leader might function as a molecular switch, which changes the fate of the viral genomic RNA from translation to packaging mode (12, 45). In agreement with this possibility, the 5′ leader of the full-length RNA can adopt two mutually exclusive secondary structures, defined as the branched multiple hairpin and the long-distance interaction structures (43–45). The

branched multiple hairpin promotes the formation of the primer-binding site, dimer initiation site, splice donor, and Ψ hairpin loops, while the long-distance interaction structure engenders alternative base pairing that disrupts the dimer initiation site hairpin loop (44, 45). Consequently, the two conformations differ in their ability to confer RNA dimer formation.

The downstream 290 to 352 region, including the *gag* start codon (nucleotides 336 to 338), also folds differently depending on the long-distance interaction and branched multiple hairpin structures. Nucleotides 334 to 344 form part of an extended hairpin structure in the long-distance interaction conformation (43–45), whereas in the branched multiple hairpin structure, this sequence engages in a novel base-pairing with the upstream U5 region (nucleotides 105 to 115), which is named the U5-AUG duplex (1). The formation of the U5-AUG duplex occludes the *gag* start codon, potentially preventing translation of the Gag protein (1). These findings explain our observations. When the *gag* coding region is appended to the IRES in the bicistronic constructs, IRES-mediated translation initiation decreased despite the fact that the RNA was stabilized (unpublished observations; see also Fig. 3 and 4, constructs 1-384, 1-504, 1-996, and 1-1836). Thus, it is conceivable that by adding part of the *gag* ORF, the formation of the U5-AUG duplex is favored, leading to inhibition of translation.

Based on the mapping data showing that the IRES overlaps the core viral packaging signal (Fig. 5), it is highly probable that changes in the IRES structure and its activity are decisive in determining the fate of full-length viral RNA, as was proposed for poliovirus (36) and Rous sarcoma virus (17, 31). Better understanding of HIV-1 IRES regulation should lead to the design of drugs which will specifically inhibit viral replication.

ACKNOWLEDGMENTS

Ann Brasey and Marcelo López-Lastra contributed equally to this work.

We thank Guylaine Roy and Andrea Brueschke for critical reading of the manuscript, S. J. Morley and V. M. Pain for the foot-and-mouth disease virus L protease, and F. L. Cosset for the TeFly-A helper cell line. We thank Damian Purcell for running the Macfarlane Burnet Centre Mfold server.

This study was supported by a grant from the Canadian Institute of Health Research (CIHR) and the American Foundation for AIDS Research to N.S. (AmFAR 02827-30-RG) and grants from NWO-CW, INSERM, and the Agence Nationale de Recherche sur le Sida (ANRS). A.B. was supported by the CIHR and a joint program of the Fonds pour la Formation de Chercheurs et l'Aide à la Recherche (FCAR) and the Fonds de la Recherche en Santé du Québec (FRSQ). M.L.-L. was supported by a CIHR postdoctoral fellowship, and T.O. was supported by the Fondation pour la Recherche Médicale. N.S. is a James McGill Professor, a CIHR Distinguished Scientist, and a Howard Hughes Medical Institute International Scholar.

REFERENCES

1. **Abbink, T. E., and B. Berkhout.** A novel long-distance base-pairing interaction in human immunodeficiency virus type 1 RNA occludes the *gag* start codon. J. Biol. Chem., in press.
2. **Adachi, A., H. E. Gendelman, S. Koenig, T. Folks, R. Willey, A. Rabson, and M. A. Martin.** 1986. Production of acquired immunodeficiency syndrome-associated retrovirus in human and nonhuman cells transfected with an infectious molecular clone. J. Virol. **59:**284–291.
3. **Aldovini, A., and R. A. Young.** 1990. Mutations of RNA and protein sequences involved in human immunodeficiency virus type 1 packaging result in production of noninfectious virus. J. Virol. **64:**1920–1926.
4. **Alizon, M., S. Wain-Hobson, L. Montagnier, and P. Sonigo.** 1986. Genetic variability of the AIDS virus: nucleotide sequence analysis of two isolates from African patients. Cell **46:**63–74.
5. **Attal, J., M. C. Theron, F. Taboit, M. Cajero-Juarez, G. Kann, P. Bolifraud, and L. M. Houdebine.** 1996. The RU5 ('R') region from human leukaemia viruses (HTLV-1) contains an internal ribosome entry site (IRES)-like sequence. FEBS Lett. **392:**220–224.
6. **Bacharach, E., and S. P. Goff.** 1998. Binding of the human immunodeficiency virus type 1 *gag* protein to the viral RNA encapsidation signal in the yeast three-hybrid system. J. Virol. **72:**6944–6949.
7. **Baudin, F., R. Marquet, C. Isel, J. L. Darlix, B. Ehresmann, and C. Ehresmann.** 1993. Functional sites in the 5′ region of human immunodeficiency virus type 1 RNA form defined structural domains. J. Mol. Biol. **229:**382–397.
8. **Beerens, N., F. Groot, and B. Berkhout.** 2000. Stabilization of the U5-leader stem in the HIV-1 RNA genome affects initiation and elongation of reverse transcription. Nucleic Acids Res. **28:**4130–4137.
9. **Belsham, G. J., and N. Sonenberg.** 2000. Picornavirus RNA translation: roles for cellular proteins. Trends Microbiol. **8:**330–335.
10. **Berkhout, B.** 1996. Structure and function of the human immunodeficiency virus leader RNA. Progress Nucleic Acid Res. Mol. Biol. **54:**1–34.
11. **Berkhout, B., J. van Wamel, and B. Klaver.** 1995. Requirements for DNA strand transfer during reverse transcription in mutant HIV-1 virions. J. Mol. Biol. **252:**59–69.
12. **Berkhout, B., and J. L. van Wamel.** 2000. The leader of the HIV-1 RNA genome forms a compactly folded tertiary structure. RNA **6:**282–295.
13. **Berkhout, B., and J. L. van Wamel.** 1996. Role of the dimer initiation site hairpin in replication of human immunodeficiency virus type 1. J. Virol. **70:**6723–6732.
14. **Berkowitz, R. D., J. Luban, and S. P. Goff.** 1993. Specific binding of human immunodeficiency virus type 1 gag polyprotein and nucleocapsid protein to viral RNAs detected by RNA mobility shift assays. J. Virol. **67:**7190–7200.
15. **Berlioz, C., and J. L. Darlix.** 1995. An internal ribosomal entry mechanism promotes translation of murine leukemia virus *gag* polyprotein precursors. J. Virol. **69:**2214–2222.
16. **Berlioz, C., C. Torrent, and J. L. Darlix.** 1995. An internal ribosomal entry signal in the rat VL30 region of the Harvey murine sarcoma virus leader and its use in dicistronic retroviral vectors. J. Virol. **69:**6400–6407.
17. **Bieth, E., C. Gabus, and J. L. Darlix.** 1990. A study of the dimer formation of Rous sarcoma virus RNA and of its effect on viral protein synthesis in vitro. Nucleic Acids Res. **18:**119–127.
18. **Bonneau, A. M., and N. Sonenberg.** 1987. Involvement of the 24-kDa cap-binding protein in regulation of protein synthesis in mitosis. J. Biol. Chem. **262:**11134–11139.
19. **Buck, C. B., X. Shen, M. A. Egan, T. C. Pierson, C. M. Walker, and R. F. Siliciano.** 2001. The human immunodeficiency virus type 1 *gag* gene encodes an internal ribosome entry site. J. Virol. **75:**181–191.
20. **Butsch, M., and K. Boris-Lawrie.** 2002. Destiny of unspliced retroviral RNA: ribosome and/or virion? J. Virol. **76:**3089–3094.
21. **Butsch, M., and K. Boris-Lawrie.** 2000. Translation is not required to generate virion precursor RNA in human immunodeficiency virus type 1-infected T cells. J. Virol. **74:**11531–11537.
22. **Chang, Y. N., D. J. Kenan, J. D. Keene, A. Gatignol, and K. T. Jeang.** 1994. Direct interactions between autoantigen La and human immunodeficiency virus leader RNA. J. Virol. **68:**7008–7020.
23. **Chen, C., and H. Okayama.** 1987. High-efficiency transformation of mammalian cells by plasmid DNA. Mol. Cell. Biol. **7:**2745–2752.
24. **Chen, C. Y., and P. Sarnow.** 1995. Initiation of protein synthesis by the eukaryotic translational apparatus on circular RNAs. Science **268:**415–417.
25. **Clavel, F., and J. M. Orenstein.** 1990. A mutant of human immunodeficiency virus with reduced RNA packaging and abnormal particle morphology. J. Virol. **64:**5230–5234.
26. **Clever, J., C. Sassetti, and T. G. Parslow.** 1995. RNA secondary structure and binding sites for *gag* gene products in the 5′ packaging signal of human immunodeficiency virus type 1. J. Virol. **69:**2101–2109.
27. **Clever, J. L., D. Mirandar, Jr., and T. G. Parslow.** 2002. RNA structure and packaging signals in the 5′ leader region of the human immunodeficiency virus type 1 genome. J. Virol. **76:**12381–12387.
28. **Cornelis, S., Y. Bruynooghe, G. Denecker, S. Van Huffel, S. Tinton, and R. Beyaert.** 2000. Identification and characterization of a novel cell cycle-regulated internal ribosome entry site. Mol. Cell **5:**597–605.
29. **Cosset, F. L., Y. Takeuchi, J. L. Battini, R. A. Weiss, and M. K. Collins.** 1995. High-titer packaging cells producing recombinant retroviruses resistant to human serum. J. Virol. **69:**7430–7436.
30. **Damgaard, C. K., H. Dyhr-Mikkelsen, and J. Kjems.** 1998. Mapping the RNA binding sites for human immunodeficiency virus type-1 *gag* and NC proteins within the complete HIV-1 and -2 untranslated leader regions. Nucleic Acids Res. **26:**3667–3676.
31. **Deffaud, C., and J. L. Darlix.** 2000. Rous sarcoma virus translation revisited: characterization of an internal ribosome entry segment in the 5′ leader of the genomic RNA. J. Virol. **74:**11581–11588.
32. **Derrington, E. A., M. Lopez-Lastra, S. Chapel-Fernandez, F. L. Cosset, M. F. Belin, B. B. Rudkin, and J. L. Darlix.** 1999. Retroviral vectors for the expression of two genes in human multipotent neural precursors and their differentiated neuronal and glial progeny. Hum. Gene Ther. **10:**1129–1138.
33. **Dorman, N., and A. Lever.** 2000. Comparison of viral genomic RNA sorting

mechanisms in human immunodeficiency virus type 1 (HIV-1), HIV-2, and Moloney murine leukemia virus. J. Virol. **74:**11413–11417.
34. **Elder, R. T., M. Yu, M. Chen, S. Edelson, and Y. Zhao.** 2000. Cell cycle G_2 arrest induced by HIV-1 Vpr in fission yeast (Schizosaccharomyces pombe) is independent of cell death and early genes in the DNA damage checkpoint. Virus Res. **68:**161–173.
35. **Emerman, M.** 1996. HIV-1, Vpr and the cell cycle. Curr. Biol. **6:**1096–1103.
36. **Gamarnik, A. V., and R. Andino.** 1998. Switch from translation to RNA replication in a positive-stranded RNA virus. Genes Dev. **12:**2293–2304.
37. **Goh, W. C., M. E. Rogel, C. M. Kinsey, S. F. Michael, P. N. Fultz, M. A. Nowak, B. H. Hahn, and M. Emerman.** 1998. HIV-1 Vpr increases viral expression by manipulation of the cell cycle: a mechanism for selection of Vpr in vivo. Nat. Med. **4:**65–71.
38. **Gummuluru, S., and M. Emerman.** 1999. Cell cycle- and Vpr-mediated regulation of human immunodeficiency virus type 1 expression in primary and transformed T-cell lines. J. Virol. **73:**5422–5430.
39. **Hayashi, T., T. Shioda, Y. Iwakura, and H. Shibuta.** 1992. RNA packaging signal of human immunodeficiency virus type 1. Virology **188:**590–599.
40. **Hershey, J. W. B., and W. C. Merrick.** 2000. Pathway and mechanism of initiation of protein synthesis, p. 33–88. *In* N. Sonenberg, J. W. B. Hershey, and M. B. Mathews (ed.), Translational control of gene expression. Cold Spring Harbor Laboratory Press, Cold Spring Harbor, N.Y.
41. **Honda, M., S. Kaneko, E. Matsushita, K. Kobayashi, G. A. Abell, and S. M. Lemon.** 2000. Cell cycle regulation of hepatitis C virus internal ribosomal entry site-directed translation. Gastroenterology **118:**152–162.
42. **Huez, I., L. Creancier, S. Audigier, M. C. Gensac, A. C. Prats, and H. Prats.** 1998. Two independent internal ribosome entry sites are involved in translation initiation of vascular endothelial growth factor mRNA. Mol. Cell. Biol. **18:**6178–6190.
43. **Huthoff, H., and B. Berkhout.** 2002. Multiple secondary structure rearrangements during HIV-1 RNA dimerization. Biochemistry **41:**10439–10445.
44. **Huthoff, H., and B. Berkhout.** 2001. Mutations in the *trans*-activation-responsive region hairpin affect the equilibrium between alternative conformations of the HIV-1 leader RNA. Nucleic Acids Res. **29:**2594–2600.
45. **Huthoff, H., and B. Berkhout.** 2001. Two alternating structures of the HIV-1 leader RNA. RNA **7:**143–157.
46. **Jang, S. K., H. G. Krausslich, M. J. Nicklin, G. M. Duke, A. C. Palmenberg, and E. Wimmer.** 1988. A segment of the 5′ nontranslated region of encephalomyocarditis virus RNA directs internal entry of ribosomes during in vitro translation. J. Virol. **62:**2636–2643.
47. **Kaye, J. F., and A. M. Lever.** 1999. Human immunodeficiency virus types 1 and 2 differ in the predominant mechanism used for selection of genomic RNA for encapsidation. J. Virol. **73:**3023–3031.
48. **Kaye, J. F., and A. M. Lever.** 1998. Nonreciprocal packaging of human immunodeficiency virus type 1 and type 2 RNA: a possible role for the p2 domain of *gag* in RNA encapsidation. J. Virol. **72:**5877–5885.
49. **Kaye, J. F., and A. M. Lever.** 1996. trans-acting proteins involved in RNA encapsidation and viral assembly in human immunodeficiency virus type 1. J. Virol. **70:**880–886.
50. **Klaver, B., and B. Berkhout.** 1994. Comparison of 5′ and 3′ long terminal repeat promoter function in human immunodeficiency virus. J. Virol. **68:** 3830–3840.
51. **Lever, A., H. Gottlinger, W. Haseltine, and J. Sodroski.** 1989. Identification of a sequence required for efficient packaging of human immunodeficiency virus type 1 RNA into virions. J. Virol. **63:**4085–4087.
52. **Lopez-Lastra, M., C. Gabus, and J. L. Darlix.** 1997. Characterization of an internal ribosomal entry segment within the 5′ leader of avian reticuloendotheliosis virus type A RNA and development of novel MLV-REV-based retroviral vectors. Hum. Gene Ther. **8:**1855–1865.
53. **Lopez-Lastra, M., S. Ulrici, C. Gabus, and J. L. Darlix.** 1999. Identification of an internal ribosome entry segment in the 5′ region of the mouse VL30 retrotransposon and its use in the development of retroviral vectors. J. Virol. **73:**8393–8402.
54. **Luban, J., and S. P. Goff.** 1994. Mutational analysis of cis-acting packaging signals in human immunodeficiency virus type 1 RNA. J. Virol. **68:**3784–3793.
55. **Maddison, B., P. Marya, and S. Heaphy.** 1998. HIV-1 *gag* binds specifically to RNA stem-loops in the 5′ leader sequence. Biochim. Biophys. Acta **1398:**305–314.
56. **Masuda, M., Y. Nagai, N. Oshima, K. Tanaka, H. Murakami, H. Igarashi, and H. Okayama.** 2000. Genetic studies with the fission yeast *Schizosaccharomyces pombe* suggest involvement of *wee1*, *ppa2*, and *rad24* in induction of cell cycle arrest by human immunodeficiency virus type 1 Vpr. J. Virol. **74:**2636–2646.
57. **McBride, M. S., and A. T. Panganiban.** 1996. The human immunodeficiency virus type 1 encapsidation site is a multipartite RNA element composed of functional hairpin structures. J. Virol. **70:**2963–2973.
58. **McBride, M. S., M. D. Schwartz, and A. T. Panganiban.** 1997. Efficient encapsidation of human immunodeficiency virus type 1 vectors and further characterization of cis elements required for encapsidation. J. Virol. **71:** 4544–4554.
59. **Mouland, A. J., M. Coady, X. J. Yao, and E. A. Cohen.** 2002. Hypophosphorylation of poly(A) polymerase and increased polyadenylation activity are associated with human immunodeficiency virus type 1 Vpr expression. Virology **292:**321–330.
60. **Nanbru, C., I. Lafon, S. Audigier, M. C. Gensac, S. Vagner, G. Huez, and A. C. Prats.** 1997. Alternative translation of the proto-oncogene c-*myc* by an internal ribosome entry site. J. Biol. Chem. **272:**32061–32066.
61. **Nanbru, C., A. C. Prats, L. Droogmans, P. Defrance, G. Huez, and V. Kruys.** 2001. Translation of the human c-*myc* P0 tricistronic mRNA involves two independent internal ribosome entry sites. Oncogene **20:**4270–4280.
62. **Ohlmann, T., M. Lopez-Lastra, and J. L. Darlix.** 2000. An internal ribosome entry segment promotes translation of the simian immunodeficiency virus genomic RNA. J. Biol. Chem. **275:**11899–11906.
63. **Ohlmann, T., D. Prévôt, D. Décimo, F. Roux, J. Garin, S. J. Morley, and J. L. Darlix.** 2002. In vitro cleavage of eIF4GI but not eIF4GII by HIV-1 protease and its effects on translation in the rabbit reticulocyte lysate system. J. Mol. Biol. **318:**9–20.
64. **Ohlmann, T., M. Rau, V. M. Pain, and S. J. Morley.** 1996. The C-terminal domain of eukaryotic protein synthesis initiation factor (eIF) 4G is sufficient to support cap-independent translation in the absence of eIF4E. EMBO J. **15:**1371–1382.
65. **Paillart, J. C., L. Berthoux, M. Ottmann, J. L. Darlix, R. Marquet, B. Ehresmann, and C. Ehresmann.** 1996. A dual role of the putative RNA dimerization initiation site of human immunodeficiency virus type 1 in genomic RNA packaging and proviral DNA synthesis. J. Virol. **70:**8348–8354.
66. **Paillart, J. C., R. Marquet, E. Skripkin, C. Ehresmann, and B. Ehresmann.** 1996. Dimerization of retroviral genomic RNAs: structural and functional implications. Biochimie **78:**639–653.
67. **Parkin, N. T., E. A. Cohen, A. Darveau, C. Rosen, W. Haseltine, and N. Sonenberg.** 1988. Mutational analysis of the 5′ non-coding region of human immunodeficiency virus type 1: effects of secondary structure on translation. EMBO J. **7:**2831–2837.
68. **Peabody, D. S., S. Subramani, and P. Berg.** 1986. Effect of upstream reading frames on translation efficiency in simian virus 40 recombinants. Mol. Cell. Biol. **6:**2704–2711.
69. **Pelletier, J., G. Kaplan, V. R. Racaniello, and N. Sonenberg.** 1988. Cap-independent translation of poliovirus mRNA is conferred by sequence elements within the 5′ noncoding region. Mol. Cell. Biol. **8:**1103–1112.
70. **Pelletier, J., and N. Sonenberg.** 1985. Insertion mutagenesis to increase secondary structure within the 5′ noncoding region of a eukaryotic mRNA reduces translational efficiency. Cell **40:**515–526.
71. **Pelletier, J., and N. Sonenberg.** 1988. Internal initiation of translation of eukaryotic mRNA directed by a sequence derived from poliovirus RNA. Nature **334:**320–325.
72. **Pyronnet, S., J. Dostie, and N. Sonenberg.** 2001. Suppression of cap-dependent translation in mitosis. Genes Dev. **15:**2083–2093.
73. **Pyronnet, S., L. Pradayrol, and N. Sonenberg.** 2000. A cell cycle-dependent internal ribosome entry site. Mol. Cell **5:**607–616.
74. **Pyronnet, S., and N. Sonenberg.** 2001. Cell cycle-dependent translational control. Curr. Opin. Genet. Dev. **11:**13–18.
75. **Reicin, A. S., A. Ohagen, L. Yin, S. Hoglund, and S. P. Goff.** 1996. The role of *gag* in human immunodeficiency virus type 1 virion morphogenesis and early steps of the viral life cycle. J. Virol. **70:**8645–8652.
76. **Shen, N., L. Jette, C. Liang, M. A. Wainberg, and M. Laughrea.** 2000. Impact of human immunodeficiency virus type 1 RNA dimerization on viral infectivity and of stem-loop B on RNA dimerization and reverse transcription and dissociation of dimerization from packaging. J. Virol. **74:**5729–5735.
77. **Subbramanian, R. A., A. Kessous-Elbaz, R. Lodge, J. Forget, X. J. Yao, D. Bergeron, and E. A. Cohen.** 1998. Human immunodeficiency virus type 1 Vpr is a positive regulator of viral transcription and infectivity in primary human macrophages. J. Exp. Med. **187:**1103–1111.
78. **Svitkin, Y. V., A. Pause, and N. Sonenberg.** 1994. La autoantigen alleviates translational repression by the 5′ leader sequence of the human immunodeficiency virus type 1 mRNA. J. Virol. **68:**7001–7007.
79. **Thomas, K. R., and M. R. Capecchi.** 1986. Introduction of homologous DNA sequences into mammalian cells induces mutations in the cognate gene. Nature **324:**34–38.
80. **Vagner, S., A. Waysbort, M. Marenda, M. C. Gensac, F. Amalric, and A. C. Prats.** 1995. Alternative translation initiation of the Moloney murine leukemia virus mRNA controlled by internal ribosome entry involving the p57/PTB splicing factor. J. Biol. Chem. **270:**20376–20383.
81. **Wang, C. T., and E. Barklis.** 1993. Assembly, processing, and infectivity of human immunodeficiency virus type 1 *gag* mutants. J. Virol. **67:**4264–4273.
82. **Williams, M. A., and R. A. Lamb.** 1989. Effect of mutations and deletions in a bicistronic mRNA on the synthesis of influenza B virus NB and NA glycoproteins. J. Virol. **63:**28–35.
83. **Wilson, J. E., M. J. Powell, S. E. Hoover, and P. Sarnow.** 2000. Naturally occurring dicistronic cricket paralysis virus RNA is regulated by two internal ribosome entry sites. Mol. Cell. Biol. **20:**4990–4999.
84. **Zhang, Y., and E. Barklis.** 1997. Effects of nucleocapsid mutations on human immunodeficiency virus assembly and RNA encapsidation. J. Virol. **71:**6765–6776.
85. **Zuker, M.** 1989. On finding all suboptimal foldings of an RNA molecule. Science **244:**48–52.